

r-Adaptive Parameterization of  
Surfaces

Rhaleb Zayer    Christian Rössl  
Hans-Peter Seidel

MPI-I-2004-4-004

January 2004

FORSCHUNGSBERICHT    RESEARCHREPORT

MAX-PLANCK-INSTITUT  
FÜR  
INFORMATIK

---

Stuhlsatzenhausweg 85    66123 Saarbrücken    Germany



**Author's Address**

Rhaleb Zayer, Christian Rössl, Hans-Peter Seidel  
Computer Graphics Group  
Max-Planck-Institut Informatik  
Stuhlsatzenhausweg 85, 66123 Saarbrücken, Germany  
Email: {zayer,roessler,hpseidel}@mpi-sb.mpg.de

## **Abstract**

Surface mesh parameterization is a fundamental tool in computer graphics, required for applications like e.g. texture mapping, remeshing and morphing. Linear parameterization methods are of particular interest. Their simplicity, efficiency and robustness, enables the processing of detailed, large meshes. In practice, however, the current linear schemes are limited to producing (quasi-)conformal parameterizations and hence may suffer from considerable distortion e.g. in length and area. We present a novel approach to effectively reduce parametric distortion. Our algorithm is simple, efficient and robust, as it requires only the solution of a sparse linear system. We smoothly adapt an existing quasi-conformal parameterization with respect to different flow quantities such as areas, angles or edge lengths. Our adaptive strategy offers a flexible means for controlling distortion based on error equidistribution. We show how this method can be extended from the planar setting to spherical parameterizations, a problem which recently attracted a lot of interest.

## **Keywords**

triangular meshes, parameterization, adaptation, error equidistribution

# r-Adaptive Parameterization of Surfaces

Rhaleb Zayer, Christian Rössl and Hans-Peter Seidel

Max-Planck-Institut für Informatik, Saarbrücken, Germany

---

## Abstract

*Surface mesh parameterization is a fundamental tool in computer graphics, required for applications like e.g. texture mapping, remeshing and morphing. Linear parameterization methods are of particular interest. Their simplicity, efficiency and robustness, enables the processing of detailed, large meshes. In practice, however, the current linear schemes are limited to producing (quasi-)conformal parameterizations and hence may suffer from considerable distortion e.g. in length and area. We present a novel approach to effectively reduce parametric distortion. Our algorithm is simple, efficient and robust, as it requires only the solution of a sparse linear system. We smoothly adapt an existing quasi-conformal parameterization with respect to different flow quantities such as areas, angles or edge lengths. Our adaptive strategy offers a flexible means for controlling distortion based on error equidistribution. We show how this method can be extended from the planar setting to spherical parameterizations, a problem which recently attracted a lot of interest.*

---

## 1. Introduction

The parameterization of surfaces has received considerable attention in recent years, as it is a central operation to various applications in computer graphics such as texture mapping, remeshing and morphing. In general, a parameterization can be regarded as a bijective mapping between the surface and the parametric domain. For instance, a surface (patch) homeomorphic to a disk is mapped onto the plane, and a genus-0 surface is typically mapped onto the unit sphere. Polygonal meshes are the most common representation for surfaces and in particular for 3D data sampled from real-world objects. For this discrete, piecewise linear approximation of surfaces, the parameterization reduces to a piecewise linear mapping. In the planar configuration, the construction of this mapping can be illustrated as "flattening" a surface patch to the plane.

In general, the parameterization induces some form of distortion. Isometric or length-preserving mappings only exist for special cases, which are rare in practical applications. Most parameterization methods try to minimize distortion based on some appropriate measure. This is done to circumvent or reduce the associated negative effects of distortion like e.g. visual artifacts due to undersampling in texture mapping. Many different approaches to this problem have been proposed, often tailored for specific applications. And there is inherently no perfect solution.

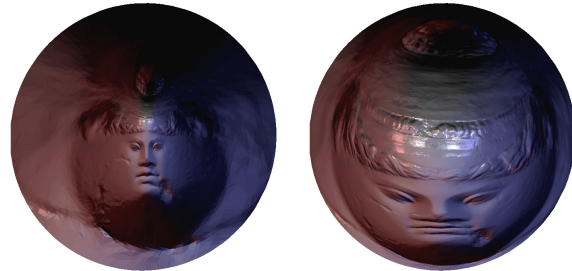


**Figure 1:** *Parameterizations of the Venus model ( $50K\Delta$ ) over the unit circle using mean value coordinates (left) and our area-adaptive method (right). The pictures visualize the flattened model with the original shading.*

Besides from providing a least-distorted mapping, an ideal parameterization method should be efficient for processing large meshes and robust, e.g. insensitive to the highly irregular input which often emerges from the digitization of real world objects. These requirements make linear parameterization methods particularly interesting. Linear methods are efficient as they only involve the solution of a sparse linear system. They have proven to be robust, and they guarantee a valid solution, given appropriate boundary conditions.

In addition, their relative simplicity and ease of implementation makes them highly attractive. Based on linear schemes, we develop a novel approach to generate low-distortion parameterizations. Our algorithm is simple, efficient and robust, it requires only the solution of a sparse linear system. We build upon the theory of mesh adaptation in order to smoothly adapt an existing (quasi-)conformal parameterization. In this process, the distortion is reduced and controlled in a flexible way through different geometric error measures (see Fig. 1). The method is independent of the parametric domain. We show how to extend it to establish spherical parameterizations of genus-0 surface meshes.

As the main contribution of this work, we provide a novel and general framework for reducing parametric distortion. The method is based on sound theory from mesh generation, namely *r*-adaptation, which to the best of our knowledge has not been applied to surface parameterization before.

The rest of the paper is organized as follows. We provide a brief overview of related work in Section 2 and describe the notion of linear mesh parameterization used throughout the paper in Section 3. A general background on *r*-adaptation methods is provided in Section 4, and we present their application to parameterization in Section 5. In Section 6 we derive the geometric error monitor functions for our approach, which is then extended to the spherical domain in Section 7. We present results and discuss the *r*-adaptive parameterization in Section 8 and conclude in Section 9.

## 2. Related work

The importance of parameterization techniques for computer graphics is reflected by the significant amount of work on the topic in the last years, see [FH03] for an extensive recent survey. Most of the research effort aims at controlling and reducing distortion through the minimization a certain deformation energy. For several approaches, the arising numerical problem is non-linear as e.g. in [HG00, SSGH01, SdS00, DMK03, ZMT04]. These methods commonly require hierarchical solvers [HGC99, SGSH02] even for moderately sized meshes and are computationally involved in general. Desbrun et al. [DMA02] use a simple non-linear optimization to linearly blend base parameterizations. An alternative approach [SCGL02] avoids global optimization problems by simultaneously cutting the surface and computing the parameterization. In this paper we consider surfaces homeomorphic to either a disk or a sphere and do not allow additional cuts. Higher genus surfaces can be partitioned into appropriate patches which are parameterized separately, see e.g. [LPRM02].

Our approach is based on linear schemes, which are commonly viewed as a physical spring analogon. Finding the equilibrium state conforms to solving the discrete Laplacian equation given appropriate boundary con-

ditions. Of particular interest are discrete conformal mappings [PP93, EDD\*95, HAT\*00] possibly with Dirichlet or Neumann boundary conditions [LPRM02, DMA02]. Most recently, Floater introduced a convex combination mapping based on the mean value theorem of harmonic functions [Flo03] as a superior alternative to his shape preserving method [Flo97]. An interesting approach was proposed by Lévy [Lév01] which allows the user to specify point constraints interactively. Yoshizawa et al. [YBS04] aim at reducing the stretch metric introduced in [SSGH01] and apply a quasi-Newton type optimization. We discuss this approach in Section 8.

The above methods flatten a surface patch homeomorphic to a disk onto the planar domain. Given a genus-0 surface, the natural parameter domain is the sphere  $S^2$ . The spherical embedding is more complex than the planar one. The difficulties arise from the additional dimension which augments the problem size and the constraint on vertices to stay on the sphere. Spherical parameterization has attracted considerable interest recently. Sheffer et al. [SGD03] extended the angle based flattening to the spherical case. Gotsman et al. [GGS03] solve a constrained problem. The reported results indicate that these are challenging optimization problems. Aiming at regular resampling of genus-0 surfaces, Praun and Hoppe [PH03] generalize the stretch metric in [SSGH01] and apply a hierarchical optimization approach.

In order to avoid an explicit constrained optimization, Kobbelt et al. [KVLS99] and Alexa [Ale00] apply an iterative, local relaxation based on uniform Laplacian smoothing and back projection onto the sphere. Gu and Yau [GY02] generate an initial uniform weights embedding which is the starting point for computing a minimal Möbius transform.

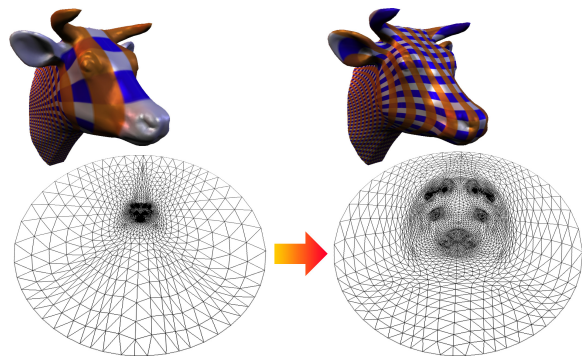


**Figure 2:** The *r*-adaptive parameterization of a surface (*r*-APS) is a two step method.: First, a (quasi-)conformal mapping is constructed (left). Second, the initial solution is adapted w.r.t. a certain deformation measure, like e.g. area distortion (right).

### 3. Notion of linear mesh parameterization

A surface is represented by a piecewise linear approximation  $\mathcal{M}$ . The triangular mesh  $\mathcal{M}$  is described as a pair  $(\mathcal{K}, X)$ , where  $\mathcal{K}$  is a simplicial complex representing the connectivity of vertices, edges and faces, and  $X = (\mathbf{x}_0, \dots, \mathbf{x}_n)$  describes the geometric positions of the vertices. We define the *1-ring neighborhood* of a vertex  $i \in \mathcal{K}$  as the set of adjacent vertices  $\mathcal{N}_i = \{j | (i, j) \in \mathcal{K}\}$ .

We represent a *parameterization* of  $\mathcal{M} = (\mathcal{K}, X)$  as an isomorphic mesh  $\mathcal{U} = (\mathcal{K}, (\mathbf{u}_1, \dots, \mathbf{u}_n))$ , where  $\mathbf{x}_i \in \mathbb{R}^3$  refer to surface points and  $\mathbf{u}_i \in \mathbb{R}^2$  denote positions in the (planar) parameter domain.

Linear parameterization schemes can be interpreted as solving the Laplace equation for a certain approximation of the discrete Laplacian operator. The approximations differ by the choice of weights  $w_{ij} \in \mathbb{R}$  if we write the Laplacian equation as

$$\mathcal{L}(\mathbf{u}_i) = \sum_{j \in \mathcal{N}_i} w_{ij}(\mathbf{u}_i - \mathbf{u}_j) = 0 \quad (1)$$

Here, we assume that the support of the Laplacian operator is restricted to the 1-ring of a vertex. Given appropriate boundary conditions, the solution of this sparse linear system for the internal vertices  $i \in \mathcal{K}$  provides their parametric positions  $\mathbf{u}_i$ . The result is guaranteed to be a one-to-one mapping if the boundary is fixed to a convex polygon in the planar domain, and if all the weights  $w_{ij}, j \in \mathcal{N}_i$  are strictly positive (see e.g. [FH03]).

### 4. Short background on r-adaptation

r-adaptation or r-refinement methods provide strategies to relocate vertex (or node) positions for adapting the mesh to best capture the behavior of a specific adaptation function. The connectivity of the mesh is fixed, so the adaptation only contracts or expands triangles (or mesh cells). These techniques are used widely in the discretization of the partial differential equations associated with fluid dynamics problems and heat transfer such as the Navier-Stokes and the Poisson equations. The driving force behind all these methods is the idea of error equidistribution. In other words, an error or energy function is made equal over all mesh elements rather than being minimized directly.

A direct error minimization approach would try to solve the associated optimization problem to find optimal positions of the vertices. Depending on the problem setting, this can be very challenging and computationally expensive. In contrast, an r-adaptation method does not directly minimize the error, but instead relocates the vertices to equidistribute the error over the domain. Naturally, this equidistribution will minimize the average global error.

This approach was first established by Babuška and Rheinboldt [BR78] in the context of finite elements computations. They proved that if some error measure is evenly dis-

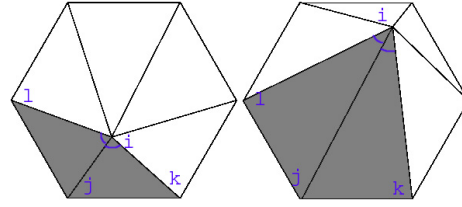


**Figure 3:** Our *r*-adaptation approach relocates a vertex  $i$  according to its 1-ring  $\mathcal{N}_i$  (Section 4). The highlighted triangles and angles are used to compute the errors  $e_{ij}^{area}$  and  $e_{ij}^{angle}$  for their common edge  $(i, j) \in \mathcal{K}$  (Section 6.4).

tributed over the mesh then the spatial distribution of nodes is asymptotically optimal (see Section 8) with respect to this measure. In particular, there is no need to locate the optimal nodal positions exactly, because the optimum error exhibits stable behavior under perturbation of the vertex positions. Technically, the method first establishes a preliminary solution, and it then attempts to relocate grid points so that a certain flow quantity, defined by an *error monitor*, is equally distributed over the field. We refer to [TWM85] for an introductory textbook on these adaptation methods.

The field of r-adaptation techniques is rich of interesting theoretical and applied results, see e.g. [Bak97] for a survey. Most of the schemes proposed in the literature are closely tied to the specific physical problems that they are designed for, and hence they may not be applicable to more general settings.

An efficient approach to node movement is repositioning each node according to its 1-ring neighborhood [Cap95, Bai02]. Let  $\mathbf{u}_i$  be the position of the vertex  $i$ . With each edge  $(i, j) \in \mathcal{K}$ , we associate a strictly positive weight  $W_{ij}$ . Assume a quantity  $Q = W_{ij} \|\mathbf{u}_i - \mathbf{u}_j\|^2, j \in \mathcal{N}_i$  is to be evenly distributed over the 1-ring. This is attained when

$$\mathcal{L}(\mathbf{u}_i) = \sum_{j \in \mathcal{N}_i} W_{ij}(\mathbf{u}_i - \mathbf{u}_j) = 0 .$$

The equidistribution over the whole mesh leads to a sparse matrix equation similar to the Laplace equation. However in this context, the weights are tuned to furnish an efficient means for adapting the mesh. Suppose the weights associated with the edges  $(i, j), (i, k)$  and  $(i, l)$  are smaller than all other weights in Fig. 3. In order to reach an even distribution of the entity  $Q$  over the ring, the central vertex position  $\mathbf{u}_i$  should move away from  $\mathbf{u}_j, \mathbf{u}_k$ , and  $\mathbf{u}_l$ . If we think of the weights as functions associated with a certain error monitor or flow quantity  $Q$ , we can perceive that the central node moved in the direction of higher  $Q$ . This implies that the existing mesh points are redistributed in order to resolve regions of high gradient.

In the following, we develop a geometric r-adaptive tech-

nique for mesh parameterization. We propose a set of error monitor functions which capture geometric distortion, and we show how to equidistribute these error measures smoothly and efficiently for the planar configuration.

## 5. *r*-adaptive parameterization

In order to drastically reduce the amount of parametric distortion without the need for solving non-linear systems, we follow the central idea of *r*-adaptation. We proceed in two steps. First, we compute an initial parameterization. Second, we adapt it and relocate its vertex positions such that the distortion is equally and smoothly distributed. Both steps can be modeled by a linear system and hence performed efficiently. Fig. 2 illustrates our approach.

In the first step, we construct a quasi-conformal parameterization based on the mean value coordinates [Flo03]. We discuss this choice of weights  $w_{ij}$  for solving (1) in Section 6.4. The averaging property of the Laplacian typically yields regions of high distortion in scale noticeable as triangle crowding. However, the conformality provides parametric triangles in  $\mathcal{U}$  which are nearly mathematically similar to the triangles of the original mesh  $\mathcal{M}$ , i.e. they are only minimally sheared. So we can regard the quasi-conformal mapping a good initial solution to the adaptive parameterization problem.

In the second step, we choose an appropriate error monitor to equidistribute the distortion over the whole mesh  $\mathcal{U}$ . The error monitor can be viewed as a flow quantity over the mesh. From this quantity, we derive strictly positive weights  $W_{ij}$  for every edge  $(i, j) \in \mathcal{K}$  to initiate the gradient flow. The adaptation problem can be easily solved, the equilibrium is achieved when  $\mathcal{L}(\mathbf{u}_i) = 0$  with respect to the new weights  $W_{ij}$  and for all internal vertices  $i \in \mathcal{K}$ . Hence, we solve again a sparse linear system of the same structure (1) as was required in the first step to compute the initial solution.

We described how we apply *r*-adaptation for surface parameterization, and that the relocation strategy for error equidistribution leads to a linear problem. In the next section we will derive different sets of weights corresponding to specific error monitors for efficient reduction of distortion.

## 6. Error monitor functions and adaptive weights

Many methods try to simultaneously capture all deformation aspects of the mapping in a single, highly convoluted measure of geometric distortion, which yields challenging numerical problems. These measures may correlate the natural geometric measures such as angles, area, and distance.

Instead, we construct different error monitor functions which provide different measures of parametric distortion. These error measures however need to satisfy certain quality criteria. We require the error measure to be strictly positive and strictly monotone, in order to resolve high gradient regions. For instance, squared difference errors which

are commonly used to set up optimization problems are not of interest to our setting as they are not strictly monotone. We will rely on these properties in Section 6.4. Experiments with many possible error functions suggest that the simplest ones yield satisfactory results in practice. Sections 6.1–6.3 describe the different error quantities  $e_{ij}$  associated with the edges  $(i, j) \in \mathcal{K}$ . Section 6.4 then discusses the derivation of the a-posteriori *r*-adaptive weights  $W_{ij}$ .

### 6.1. Area-based error monitor

Generally existing conformal parameterizations tend to scale triangles. The scaling factor typically increases from the boundary to the interior of the mesh. Fig 2 illustrates this effect. Regarding a single triangle, it seems natural to formulate an error monitor in terms of its area measured in 3D and in parametric space. We define the area error of a triangle  $(i, j, k) \in \mathcal{K}$  as

$$e_{ijk}^{\text{area}} = \frac{\text{area}(\mathbf{u}_i, \mathbf{u}_j, \mathbf{u}_k)}{\text{area}(\mathbf{x}_i, \mathbf{x}_j, \mathbf{x}_k)},$$

i.e. the ratio of areas of the planar conformal triangle and the 3D surface triangle. Note that this error is strictly monotone and positive as required.

We define the error on each edge  $(i, j) \in \mathcal{K}$  as the average error of the adjacent triangles  $(i, j, k)$  and  $(j, i, l)$  (see Fig. 3), i.e.

$$e_{ij}^{\text{area}} = \frac{e_{ijk} + e_{jil}}{2}, \quad (i, j, k), (j, i, l) \in \mathcal{K}$$

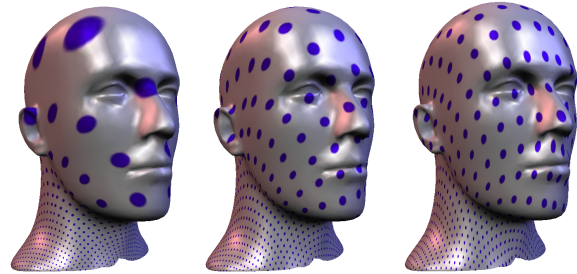


**Figure 5:** Visualization of the parameterization of the Mannequin head ( $21K\Delta$ ) using mean value coordinates (left), and *r*-APS with edge-length adaptive weights for different exponents  $\alpha = 1$  (center) and  $\alpha = \frac{3}{2}$  (right).

### 6.2. Edge length error monitor

In a similar fashion we define an error monitor based on edge lengths. The error associated with an edge  $(i, j) \in \mathcal{K}$  is simply defined as the ratio of the planar edge lengths over the length of the original edge in 3D, hence

$$e_{ij}^{\text{length}} = \frac{\|\mathbf{u}_i - \mathbf{u}_j\|}{\|\mathbf{x}_i - \mathbf{x}_j\|}.$$



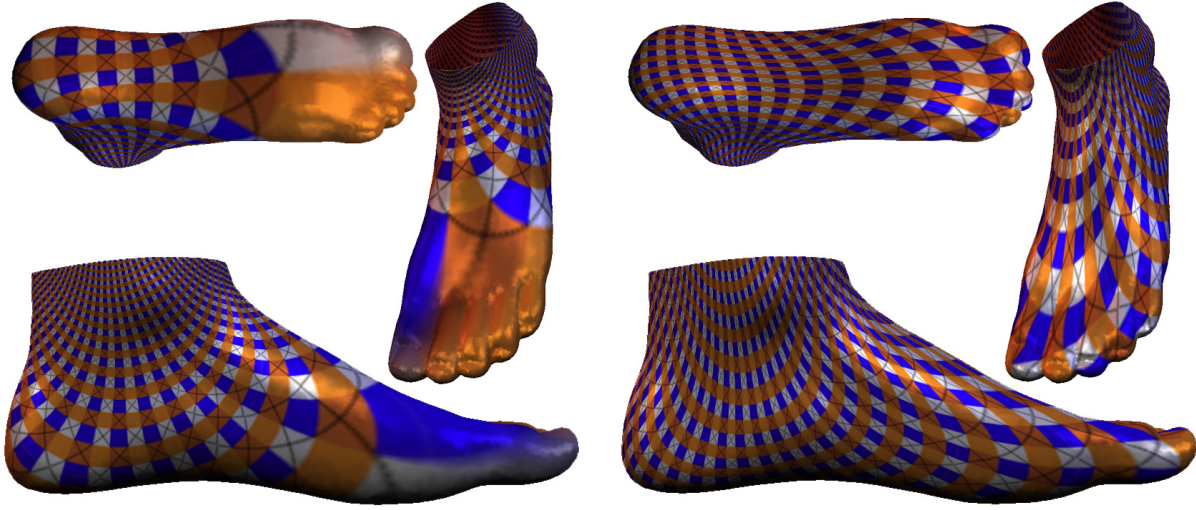


**Figure 4:** Parameterization of the Foot model ( $20K\Delta$ ) using mean value weights (left) and r-APS with the a posteriori area-adaptive weights (right). Such kind of "sock-like" surfaces typically induce high distortion and hence pose a challenging problem. The parameterization is visualized by mapping a regular texture. The different views show how the distortion is equally distributed over the whole mesh and how the r-APS tends to preserve the conformality of the initial solution (see also Figures 9 (right) and 10).

Although very simple, this error function offers a nice mathematical interpretation. Given are two metrics  $(S, d)$  and  $(S', d')$  and a map  $f : S \rightarrow S'$ . It is well known from basic analysis that the contraction of  $f$  is the maximum factor by which distances are shrunk, i.e.

$$\max_{p, q \in S} \frac{d(p, q)}{d'(f(p), f(q))}.$$

On the other hand, the expansion is the maximum factor by which distances are stretched, i.e.

$$\max_{p, q \in S} \frac{d'(f(p), f(q))}{d(p, q)}.$$

The distortion of  $f$  is then defined as the product of contraction and expansion. An isometric mapping has distortion 1. From the definition of  $e_{ij}^{\text{length}}$  it is clear that after an equidistribution of the edge length error the contraction and expansion values will tend to get close to a common value. Consequently, their product and hence the distortion of the mapping will get close to 1, which means the mapping itself will be close to isometric.

### 6.3. Angle-based error monitor

Our third error monitor is designed to equidistribute the angular error of the parameterization. At first sight, it seems that this measure was needless as the initial parameterization is chosen quasi-conformal. However, a closer inspection

shows that the error induced by the respective parameterization methods is generally not evenly distributed over the surface but rather fluctuates (see Fig. 6).

We measure the angular error per triangle  $(i, j, k) \in \mathcal{K}$  and define it as the ratio

$$e_{ijk}^{\text{angle}} = \frac{\widehat{\mathbf{u}_j, \mathbf{u}_i, \mathbf{u}_k}}{\mathbf{x}_j, \mathbf{x}_i, \mathbf{x}_k}$$

The contribution to each edge  $(i, j) \in \mathcal{K}$  is then defined as the average angular error of the adjacent triangles  $(i, j, k)$  and  $(j, i, l)$ , measured at the angles incident to vertex  $i$ , i.e.

$$e_{ij}^{\text{angle}} = \frac{e_{ijk} + e_{ijl}}{2}.$$

### 6.4. Adaptive weights

We consider an error monitor with errors  $e_{ij}$  associated with edges of the mesh. Setting the weights

$$W_{ij} = e_{ij}$$

for solving the Laplacian equation effectively reduces the error and generally yields a valid parameterization because of the strictly positive weights. However, the result is not visually pleasant, as it loses smoothness, see Fig. 6 (b). The reason for this undesirable behavior is that the new weights do not take into consideration the smoothness of the solution. In an ideal setting, we would like the mapping to inherit some (or even as much as possible) of the conformality of the initial solution.

This issue is well-known in the context of adaptive grid generation [Che94] as preserving conformality smoothness. For the adaptive grid generation, this is achieved by incorporating smoothness terms in the governing partial differential equations. We propose a more straightforward approach which serves our purpose and maintains the linearity of our setting.

In order to achieve conformal smoothness, we introduce a conformality term to the adaptive weights which provides some inherent smoothness. This can be done in a simple manner setting

$$W_{ij} = w_{ij} e_{ij},$$

where the  $w_{ij}$  are the quasi-conformal weights which are also used to construct the initial mapping, in our case the mean value weights. The resulting adapted parameterizations indeed show the preservation of conformality as well as the asymptotic convergence towards the global minimum distortion (see Fig. 10 and Section 8).

Our experiments with different error functions indicate that the composition of these error monitors with strictly positive and increasing functions yields more control of their relative effect on the weights. A simple and effective example are power functions, i.e.  $W_{ij} = w_{ij} e_{ij}^\alpha$ ,  $\alpha \geq 1$ , as also applied in [DMK03, YBS04]

The results generally improve for a small exponent  $\alpha$ . However, the effect is limited as the use of high powers does not seem to reflect a natural error function anymore. Typical values for practical use range from 1 to 5, depending on the error monitor. We note that tuning the exponent  $\alpha$  affects the conditioning of the system matrix. So using an iterative solver, a higher number of iterations is required to achieve convergence. The use of preconditioners generally leads to better convergence properties.

## 7. Spherical adaptation

The error monitor functions we derived are not specific to the planar case. They can also be applied to the spherical setting, i.e. a surface mesh of genus zero is parameterized over the sphere  $S^2$ . The adaptive spherical parameterization proceeds in two steps. First, we construct an initial quasi-conformal mapping to the unit sphere. Second, we use the resulting embedding as a starting point for our adaptive scheme. Again, the adaptation strategy relocates the vertex positions in order to equidistribute the error induced by the initial quasi-conformal embedding. In contrast to the planar configuration, this is not a linear process anymore due to the constraint on the vertices to stay on the sphere. We apply an iterative relaxation algorithm, after each relocation step the vertex is projected back onto the sphere.

Our approach to generating the initial quasi-conformal parameterization derives from [GY02]. The main difference is that there is no need for an initial uniform weights mapping

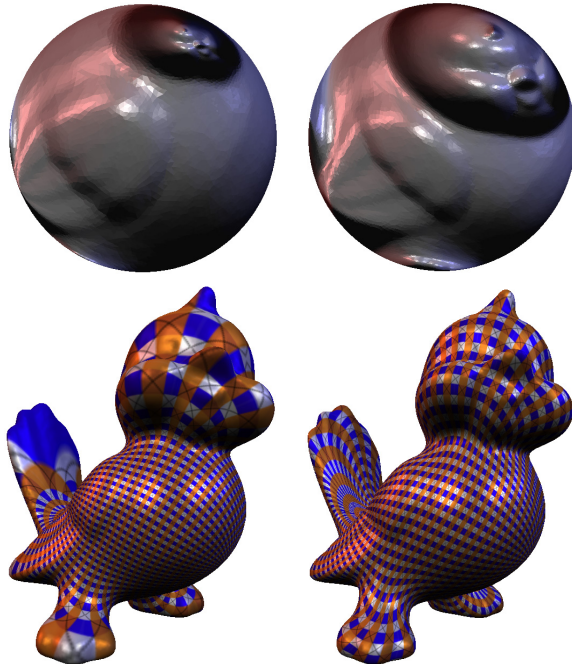


**Figure 8:** Spherical parameterizations of the Tweety model (54KΔ). The pictures show the spherical embedding (top row) and visualize the distortion by mapping a regular grid texture (bottom row). Left: Result from algorithm 7.1 using mean value coordinates. Right: *r-APS* with area-adaptive weights.

to the sphere, and our approach avoids the computation of the Möbius transform. Given an input mesh  $\mathcal{M} = (K, X)$ , our algorithm computes a spherical mapping  $\mathcal{U}$  as follows

### algorithm 7.1 (construct spherical mapping $\mathcal{U}$ of $\mathcal{M}$ )

1. Initialize  $\mathcal{U} := (K, U)$ , where  $U := X$ , i.e.  $\mathbf{u}_i \in \mathbb{R}^3$ .
2. Translate  $U$  so that  $\frac{1}{n} \sum_{i=1}^n \mathbf{u}_i = (0, 0, 0)$  (set cog origin).
3. Project the  $\mathbf{u}_i$  onto the unit sphere (Gauss map).
4. For each vertex  $i = 1, \dots, n$ 
  - $\mathcal{L}_{||}(\mathbf{u}_i) = \mathcal{L}(\mathbf{u}_i) - \langle \mathcal{L}(\mathbf{u}_i), N(\mathbf{u}_i) \rangle N(\mathbf{u}_i)$   
(tangential component of the Laplacian)
  - $\mathbf{u}_i := \mathbf{u}_i + \lambda \mathcal{L}_{||}(\mathbf{u}_i)$  (update)
  - $\mathbf{u}_i := \mathbf{u}_i / \|\mathbf{u}_i\|$  (back projection)
5. Repeat step (4.) until convergence.

Here,  $N(\mathbf{u}_i) = \mathbf{u}_i / \|\mathbf{u}_i\|$  denotes the unit normal vector of vertex  $i$ , and  $\lambda \in (0, 1]$  is a damping coefficient.

Once the above algorithm has converged, we can adapt the quasi-conformal solution by iterating step (4.) with the adaptive weights (cf. Section 6.4) for computing the Laplacian  $\mathcal{L}(\mathbf{u}_i)$ .

Our method is practical even for fairly complex meshes (see Fig. 7 and 8) without auxiliary hierarchies. However,

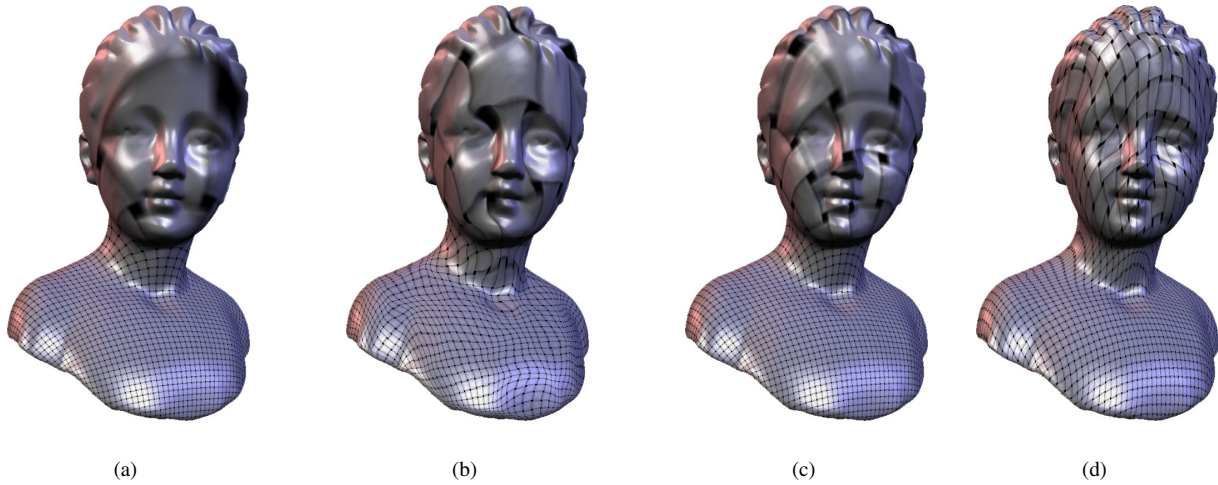


**Figure 6:** *r*-APS with different adaptation strategies applied to a bust model ( $47K\Delta$ ). (a) Initial solution from mean-value coordinates. (b) Solution from angle-adaptive weights without conformality smoothness term, note the irregularity of the solution. *r*-APS with angle-adaptive weights for exponent  $\alpha = 1$  (c) and  $\alpha = 5$  (d).

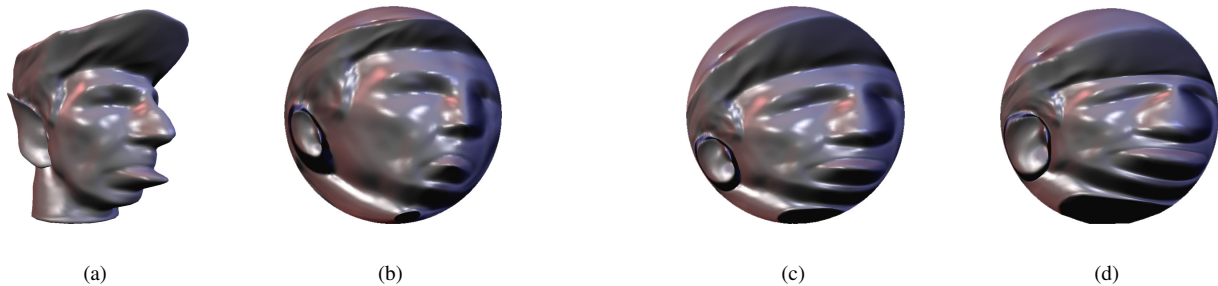


**Figure 7:** Spherical parameterizations of an edited head model ( $33K\Delta$ ), the edit (a) amplifies the distortion problem. (b) initial conformal mapping generated by algorithm 7.1. *r*-APS embeddings using area-adaptive weights for different exponents  $\alpha = 1$  (c) and  $\alpha = 2$  (d).

the algorithm is limited by the approximation of the Laplacian operator on the sphere, which assumes that the 1-ring of each vertex  $i$  can be considered as quasi-planar. We note that this limitation is inherent to all parameterization methods based on the tangential Laplacian. The approximation error induced by this assumption is of the order of  $\theta \approx \sin(\theta)$ , where  $\theta$  denotes the angle of an incident edge  $(i, j) \in \mathcal{K}$  with the tangent plane to the sphere at the center  $\mathbf{u}_i$  of the 1-ring. If  $\theta$  gets large, the vertices will tend to cluster in a region on the sphere. In practice, this effect may be controlled by tuning the damping coefficient  $\lambda$  or locally refining the mesh connectivity.

## 8. Results and discussion

We applied our *r*-adaptive parameterization method to a variety of reasonably complex geometric models, for both, the planar and the spherical setting. The Figures 1, 4-6 and 7-

8 and 12 show examples for different configurations. In our implementation we use a bi-conjugate gradient algorithm to solve the linear systems for the planar configuration. The computation times are in the order of seconds as it is typical for solving this class of problems on current hardware. The times are in the order of seconds to minutes for the spherical parameterization, which is dominated by the computation of the initial quasi-conformal embedding. We do not apply any auxiliary hierarchies. The implementation of the *r*-adaptive methods is relatively simple, and in particular the extension of an existing linear parameterization scheme to our *r*-adaptive algorithm is straightforward, and hence our results can be easily reproduced.

**Asymptotic optimality of *r*-adaptation.** As mentioned in Section 4, the error equidistribution yields an asymptotically optimal distribution of vertex positions with respect to the desired flow quantity. Fig. 9 (right) illustrates the asymptotic

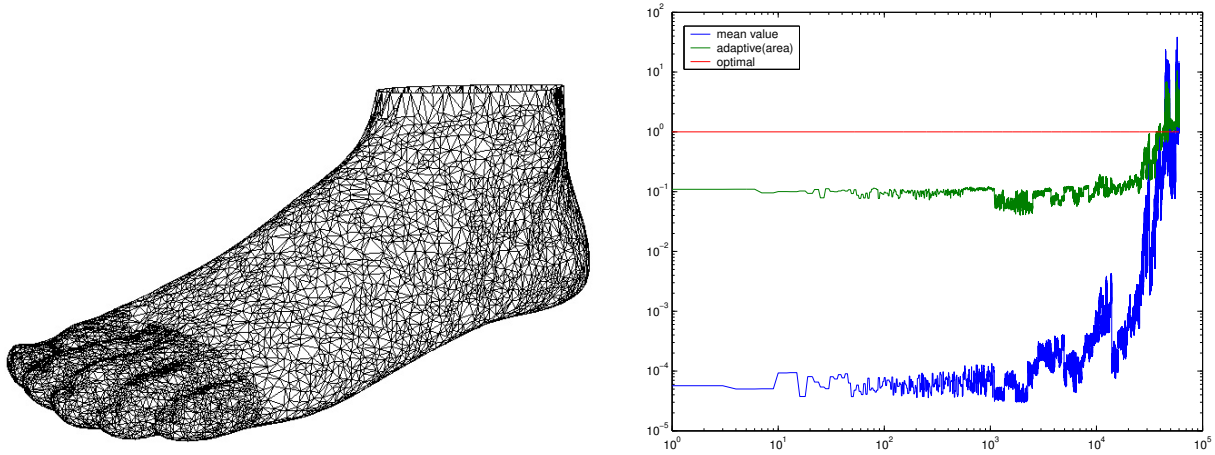


**Figure 9:** Left: The tessellation of the Foot surface (cf. Fig. 4) is very irregular, the *r*-APS algorithm robustly processes this input due to the positivity of the adaptive weights derived from mean value coordinates. Right: Normalized area distortion error  $e_{ijk}^{area}$  for the Foot model. The triangles  $(i, j, k) \in \mathcal{K}$  are enumerated over the horizontal axis. And the vertical axis measures the error for each triangle. Note that the scales are logarithmic for better visualization.

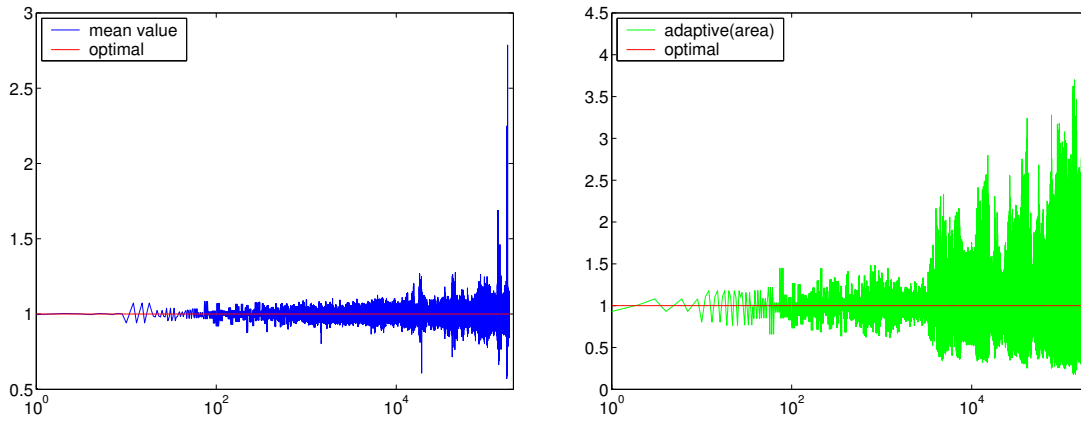


**Figure 10:** Angular error of the initial mean value coordinates solution (left) and the area adaptive *r*-APS (right) for the Foot model. The logarithmic horizontal axis enumerates the triangles. The graphs indicate that the *r*-APS tends to preserve the conformality of the initial solution as the area adaptive solution mimics the asymptotic behavior of the initial quasi-conformal solution.

convergence of our *r*-adaptive parameterization for the area-based error monitor. The graph compares the area distortion error  $e_{ijk}^{area}$  over all triangles  $(i, j, k) \in \mathcal{K}$  for the mean value coordinates and for the adaptive parameterization, which is asymptotic to the optimum 1.

**Conformality smoothness.** Fig. 10 opposes the angular errors  $e_{ijk}^{angular}$  of the initial solution to the result of area adaptation (as before). This indicates that the adaptive parameterization tends to preserve the conformality of the initial mean value coordinates solution. We observed that the smoothness of the solution is altered, if highly convoluted measures (see

also Section 6.4) like [SSGH01] are used for deriving error monitor functions.

**Choice of quasi-conformal weights.** We opt for the mean value coordinates as quasi-conformal weights due to their positivity which guarantees a valid mapping (see also [FHK04] for a detailed analysis), and because they provide good results in practice. In contrast, the positivity of the discrete conformal weights [PP93, DMA02] is generally guaranteed only for Delaunay triangulations. However, for arbitrary triangulations, the sum of these weights over the 1-ring is positive [Win66]. While this method can converge with some weights being negative, we note that coupling

them with our adaptive scheme might render them unstable. This is due to the fact that the sum over the 1-ring may become negative, which propagates the negativity over the ring. Fig. 9 (left) shows an irregular mesh which causes this effect. The problem could be fixed by locally refining the mesh connectivity. We observed that if the adapted discrete conformal system converges, the solution tends to be better than the (harmonic) mean value coordinates embedding. Fig. 11 shows an example of our adaptation coupled with the discrete conformal weights. Note the preservation of the symmetry despite the irregularity of the sampling.

**Alternative linear methods.** Desbrun et al. [DMA02] derive the discrete authalic parameterization which is locally area preserving. This property seems not to be sufficient to achieve a global reduction of area distortion. Consequently, also the effect of blending between a discrete conformal and an authalic base parameterization is limited. The same work enables an interesting approach to optimizing the mesh boundary in a postprocess in order to improve on distortion. An alternative method [Lév01] fixes internal points and extrapolates the solution to reduce parametric distortion. Both of the above issues could possibly be addressed by r-adaptation in the future.

**Non-linear methods.** Many of the non-linear approaches [SSGH01, HG00] use an initial embedding as starting point and then try to optimize it with respect to some deformation energy by performing a local random line search until a certain threshold is achieved. Most recently, Yoshizawa et al. [YBS04] minimize the stretch metric from [SSGH01] starting from an initial shape preserving [Flo97] mapping. The optimization procedure performs a multi-step search along the line of decreasing stretch. The solution in every step is obtained by solving a linear system where the weights are tuned according to the stretch metric. As there is no guarantee of convergence, the method stops when the global stretch increases instead of decreasing, and the last step is considered as the optimal solution. While the linear system solved in every step bears similarity to Winslow’s variable diffusion technique [Bra93] tailored to the stretch metric, there is no guarantee to find an optimal solution due to the non-convexity of the optimization problem. [YBS04] note that a lower stretch parameterization does not necessarily account for a visually better mapping. This is partly due to the nature of the stretch metric functional, as it convolutes two terms that reflect change in both length and area. In contrast to heuristic direct minimization approaches, we provide a general framework which features provable guarantees like smoothness of the solution and asymptotic convergence to the optimal solution thanks to sound theory. Hence, our approach is fundamentally different from Newton-type optimization methods. We strictly apply an error equidistribution to indirectly reduce the distortion according to several non-convoluted error monitor functions applying only *one* single linear system on top of the initial solution. Furthermore our approach easily extends to higher dimensions.

## 9. Conclusion

We presented a novel approach to surface mesh parameterization. Our method is inspired by and builds upon r-adaptation, which is a general technique to relocate the vertex positions according to a certain error measure. We apply a linear relocation strategy for the equidistribution of parametric distortion, which makes our r-adaptive parameterization of surfaces simple, efficient and robust. The coefficients of the sparse linear system are carefully derived, which guarantees convergence and maintains the smoothness of the solution. The proposed error monitor functions provide flexible means to control distortion, they can be directly applied to existing parameterization methods, and they are not restricted to the planar domain. So far, we considered fixed, convex boundaries in order to guarantee a valid mapping. Yet, there is no reason indicating why our approach could not be coupled with suitable Dirichlet or Neumann boundary conditions or a posteriori optimization of the boundary. This issue will be subject of future work.

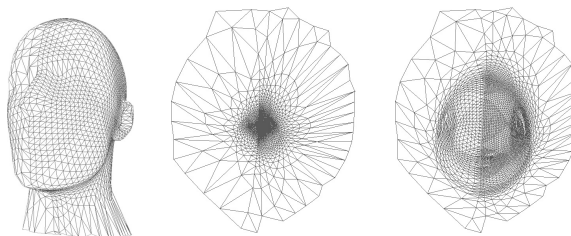


**Figure 11:** Parameterization of the well-known irregularly sampled head [DMA02]. We adapt the discrete conformal parameterization with natural boundaries (center) using edge-length adaptive weights with exponent  $\alpha = 2$  (right).

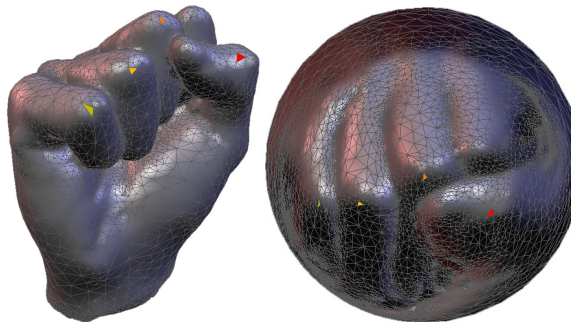


**Figure 12:** Edge-length adaptive spherical embedding of a Fist model (14K $\Delta$ ), four triangles on the fingers are consistently highlighted.

## References

- [Ale00] ALEXA M.: Merging polyhedral shapes with scattered features. In *The Visual Computer*, vol. 16(1). Springer, 2000, pp. 26–37. 2

- [Bai02] BAINES M. J.: Moving meshes, conservation laws and least squares equidistribution. *Internat. J. Numer. Methods Fluids* 40, 1-2 (2002), 3–19. ICFD Conference on Numerical Methods for Fluid Dynamics (Oxford, 2001). 3
- [Bak97] BAKER T. J.: Mesh adaptation strategies for problems in fluid dynamics. *Finite Elem. Anal. Des.* 25, 3-4 (1997), 243–273. 3
- [BR78] BABUŠKA I., RHEINBOLDT W. C.: Error estimates for adaptive finite element computations. *SIAM J. Numer. Anal.* 15, 4 (1978), 736–754. 3
- [Bra93] BRACKBILL J. U.: An adaptive grid with directional control. *J. Comput. Phys.* 108, 1 (1993), 38–50. 9
- [Cap95] CAPON P.: *Adaptive Stable Finite Element Methods for the Compressible Navier-Stokes Equations*. PhD thesis, School of Computer Studies, University of Leeds, 1995. 3
- [Che94] CHEN K.: Two dimensional adaptive quadrilateral mesh generation. *Comm. Numer. Meth. Eng.* 10 (1994). 6
- [DMA02] DESBRUN M., MEYER M., ALLIEZ P.: Intrinsic parameterizations of surface meshes. *Computer Graphics Forum (Proc. Eurographics)* 21, 3 (2002), 209–218. 2, 8, 9
- [DMK03] DEGENER P., MESETH J., KLEIN R.: An adaptable surface parameterization method. *Proc. 9th International Meshing Roundtable* (2003), 201–213. 2, 6
- [EDD\*95] ECK M., DEROSE T., DUCHAMP T., HOPPE H., LOUNSBERRY M., STUETZLE W.: Multiresolution analysis of arbitrary meshes. *Computer Graphics (Proc. SIGGRAPH)* 29 (1995), 173–182. 2
- [FH03] FLOATER M. S., HORMANN K.: Recent advances in surface parameterization. In *Proc. Multiresolution in Geometric Modelling* (Cambridge, UK, 2003), pp. 259–284. 2, 3
- [FHK04] FLOATER M. S., HORMANN K., KÓS G.: A general construction of barycentric coordinates over convex polygons. *Advances in Computational Mathematics (preprint)* (2004). Accepted. 8
- [Flo97] FLOATER M. S.: Parameterization and smooth approximation of surface triangulations. *Comp. Aided Geom. Design* 14, 3 (1997), 231–250. 2, 9
- [Flo03] FLOATER M. S.: Mean value coordinates. *Comput. Aided Geom. Design* 20, 1 (2003), 19–27. 2, 4
- [GGS03] GOTSMAN C., GU X., SHEFFER A.: Fundamentals of spherical parameterization for 3D meshes. *ACM Transactions on Graphics (Proc. SIGGRAPH)* 22, 3 (2003), 358–363. 2
- [GY02] GU X., YAU S.-T.: Computing conformal structures of surfaces. *Communications in Information and Systems* 2 (2002), 121–146. 2, 6
- [HAT\*00] HAKER S., ANGENENT S., TANNENBAUM A., KIKINIS R., SAPIRO G., HALLE M.: Conformal surface parameterization for texture mapping. *IEEE Transactions on Visualization and Computer Graphics* 6, 2 (2000), 181–189. 2
- [HG00] HORMANN K., GREINER G.: MIPS: An efficient global parameterization method. In *Curve and Surface Design: Saint-Malo 1999*, Laurent P.-J., Sablonnière P., Schumaker L. L., (Eds.). Vanderbilt University Press, 2000, pp. 153–162. 2, 9
- [HGC99] HORMANN K., GREINER G., CAMPAGNA S.: Hierarchical parameterization of triangulated surfaces. In *Proceedings of Vision, Modeling, and Visualization* (1999), pp. 219–226. 2
- [KVLS99] KOBBELT L., VORSATZ J., LABSIK U., SEIDEL H.-P.: A shrink wrapping approach to remeshing polygonal surfaces. *Computer Graphics Forum (Proc. Eurographics)* 18, 3 (1999), 119–130. 2
- [Lév01] LÉVY B.: Constrained texture mapping for polygonal meshes. In *Computer Graphics (Proc. SIGGRAPH)* (2001), pp. 417–424. 2, 9
- [LPRM02] LÉVY B., PETITJEAN S., RAY N., MAILLOT J.: Least squares conformal maps for automatic texture atlas generation. *ACM Transactions on Graphics (Proc. SIGGRAPH)* 21, 3 (2002), 362–371. 2
- [PH03] PRAUN E., HOPPE H.: Spherical parameterization and remeshing. *ACM Transactions on Graphics (Proc. SIGGRAPH)* 22, 3 (2003), 340–349. 2
- [PP93] PINKALL U., POLTHIER K.: Computing discrete minimal surfaces and their conjugates. *Experiment. Math.* 2, 1 (1993), 15–36. 2, 8
- [SCGL02] SORKINE O., COHEN-OR D., GOLDENTHAL R., LISCHINSKI D.: Bounded-distortion piecewise mesh parameterization. In *Proc. IEEE Visualization* (2002), pp. 355–362. 2
- [Sds00] SHEFFER A., DE STURLER E.: Parameterization of faceted surfaces for meshing using angle based flattening. *Engineering with Computers* 17, 3 (2000), 326–337. 2
- [SGD03] SHEFFER A., GOTSMAN C., DYN N.: Robust spherical parameterization of triangular meshes. In *Proc. of 4th Israel-Korea Binational Workshop on Geometric Modeling and Computer Graphics* (2003), pp. 94–99. 2
- [SGSH02] SANDER P. V., GORTLER S. J., SNYDER J., HOPPE H.: Signal-specialized parameterization. In *Eurographics Workshop on Rendering* (2002), pp. 87–98. 2
- [SSGH01] SANDER P. V., SNYDER J., GORTLER S. J., HOPPE H.: Texture mapping progressive meshes. In *Computer Graphics (Proc. SIGGRAPH)* (2001), pp. 409–416. 2, 8, 9
- [TWM85] THOMPSON J. F., WARSI Z. U. A., MASTIN C. W.: *Numerical grid generation*. North-Holland Publishing Co., New York, 1985. 3
- [Win66] WINSLOW A. M.: Numerical solution of the quasilinear Poisson equation in a nonuniform triangle mesh. *J. of Computational Physics* 1, 2 (1966), 149–172. 8
- [YBS04] YOSHIKAWA S., BELYAEV A. G., SEIDEL H.-P.: A fast and simple stretch-minimizing mesh parameterization. In *Proc. Shape Modeling International* (2004), p. to appear. 2, 6, 9
- [ZMT04] ZHANG E., MISCHAIKOW K., TURK G.: Feature-based surface parameterization and texture mapping. (*preprint available as technical report*) (2004). 2



Below you find a list of the most recent technical reports of the Max-Planck-Institut für Informatik. They are available by anonymous ftp from [ftp.mpi-sb.mpg.de](ftp://ftp.mpi-sb.mpg.de) under the directory `pub/papers/reports`. Most of the reports are also accessible via WWW using the URL <http://www.mpi-sb.mpg.de>. If you have any questions concerning ftp or WWW access, please contact [reports@mpi-sb.mpg.de](mailto:reports@mpi-sb.mpg.de). Paper copies (which are not necessarily free of charge) can be ordered either by regular mail or by e-mail at the address below.

Max-Planck-Institut für Informatik  
 Library  
 attn. Anja Becker  
 Stuhlsatzenhausweg 85  
 66123 Saarbrücken  
 GERMANY  
 e-mail: [library@mpi-sb.mpg.de](mailto:library@mpi-sb.mpg.de)

MPI-I-2004-NWG3-001	M. Magnor	Axisymmetric Reconstruction and 3D Visualization of Bipolar Planetary Nebulae
MPI-I-2004-5-001	S. Siersdorfer, S. Sizov, G. Weikum	Goal-oriented Methods and Meta Methods for Document Classification and their Parameter Tuning
MPI-I-2004-4-003	Y. Ohtake, A. Belyaev, H. Seidel	3D Scattered Data Interpolation and Approximation with Multilevel Compactly Supported RBFs
MPI-I-2004-4-002	Y. Ohtake, A. Belyaev, H. Seidel	Quadric-Based Mesh Reconstruction from Scattered Data
MPI-I-2004-4-001	J. Haber, C. Schmitt, M. Koster, H. Seidel	Modeling Hair using a Wisp Hair Model
MPI-I-2004-2-001	H.d. Nivelles, Y. Kazakov	Resolution Decision Procedures for the Guarded Fragment with Transitive Guards
MPI-I-2004-1-004	N. Sivadasan, P. Sanders, M. Skutella	Online Scheduling with Bounded Migration
MPI-I-2004-1-003	I. Katriel	On Algorithms for Online Topological Ordering and Sorting
MPI-I-2004-1-002	P. Sanders, S. Pettie	A Simpler Linear Time $2/3 - \epsilon$ Approximation for Maximum Weight Matching
MPI-I-2004-1-001	N. Beldiceanu, I. Katriel, S. Thiel	Filtering algorithms for the Same and UsedBy constraints
MPI-I-2004-	R. Zayer	?
MPI-I-2003-NWG2-002	F. Eisenbrand	Fast integer programming in fixed dimension
MPI-I-2003-NWG2-001	L.S. Chandran, C.R. Subramanian	Girth and Treewidth
MPI-I-2003-4-009	N. Zakaria	FaceSketch: An Interface for Sketching and Coloring Cartoon Faces
MPI-I-2003-4-008	C. Roessl, I. Ivrişimţzis, H. Seidel	Tree-based triangle mesh connectivity encoding
MPI-I-2003-4-007	I. Ivrişimţzis, W. Jeong, H. Seidel	Neural Meshes: Statistical Learning Methods in Surface Reconstruction
MPI-I-2003-4-006	C. Roessl, F. Zeilfelder, G. Nrnberger, H. Seidel	Visualization of Volume Data with Quadratic Super Splines
MPI-I-2003-4-005	T. Hangelbroek, G. Nrnberger, C. Roessl, H.S. Seidel, F. Zeilfelder	The Dimension of $C^1$ Splines of Arbitrary Degree on a Tetrahedral Partition
MPI-I-2003-4-004	P. Bekaert, P. Slusallek, R. Cools, V. Havran, H. Seidel	A custom designed density estimation method for light transport
MPI-I-2003-4-003	R. Zayer, C. Roessl, H. Seidel	Convex Boundary Angle Based Flattening
MPI-I-2003-4-002	C. Theobalt, M. Li, M. Magnor, H. Seidel	A Flexible and Versatile Studio for Synchronized Multi-view Video Recording
MPI-I-2003-4-001	M. Tarini, H.P.A. Lensch, M. Goesele, H. Seidel	3D Acquisition of Mirroring Objects

MPI-I-2003-2-004	A. Podelski, A. Rybalchenko	Software Model Checking of Liveness Properties via Transition Invariants
MPI-I-2003-2-003	Y. Kazakov, H. Nivelle	Subsumption of concepts in $DL \mathcal{FL}_0$ for (cyclic) terminologies with respect to descriptive semantics is PSPACE-complete
MPI-I-2003-2-002	M. Jaeger	A Representation Theorem and Applications to Measure Selection and Noninformative Priors
MPI-I-2003-2-001	P. Maier	Compositional Circular Assume-Guarantee Rules Cannot Be Sound And Complete
MPI-I-2003-1-018	G. Schaefer	A Note on the Smoothed Complexity of the Single-Source Shortest Path Problem
MPI-I-2003-1-017	G. Schfer, S. Leonardi	Cross-Monotonic Cost Sharing Methods for Connected Facility Location Games
MPI-I-2003-1-016	G. Schfer, N. Sivadasan	Topology Matters: Smoothed Competitive Analysis of Metrical Task Systems
MPI-I-2003-1-015	A. Kovcs	Sum-Multicoloring on Paths
MPI-I-2003-1-014	G. Schfer, L. Becchetti, S. Leonardi, A. Marchetti-Spaccamela, T. Vredeveld	Average Case and Smoothed Competitive Analysis of the Multi-Level Feedback Algorithm
MPI-I-2003-1-013	I. Katriel, S. Thiel	Fast Bound Consistency for the Global Cardinality Constraint
MPI-I-2003-1-012		- not published -
MPI-I-2003-1-011	P. Krysta, A. Czumaj, B. Voecking	Selfish Traffic Allocation for Server Farms
MPI-I-2003-1-010	H. Tamaki	A linear time heuristic for the branch-decomposition of planar graphs
MPI-I-2003-1-009	B. Csaba	On the Bollobás – Eldridge conjecture for bipartite graphs
MPI-I-2003-1-008	P. Sanders	Polynomial Time Algorithms for Network Information Flow
MPI-I-2003-1-007	H. Tamaki	Alternating cycles contribution: a strategy of tour-merging for the traveling salesman problem
MPI-I-2003-1-006	M. Dietzfelbinger, H. Tamaki	On the probability of rendezvous in graphs
MPI-I-2003-1-005	M. Dietzfelbinger, P. Woelfel	Almost Random Graphs with Simple Hash Functions
MPI-I-2003-1-004	E. Althaus, T. Polzin, S.V. Daneshmand	Improving Linear Programming Approaches for the Steiner Tree Problem
MPI-I-2003-1-003	R. Beier, B. Vcking	Random Knapsack in Expected Polynomial Time
MPI-I-2003-1-002	P. Krysta, P. Sanders, B. Vcking	Scheduling and Traffic Allocation for Tasks with Bounded Splittability
MPI-I-2003-1-001	P. Sanders, R. Dementiev	Asynchronous Parallel Disk Sorting
MPI-I-2002-4-002	F. Drago, W. Martens, K. Myszkowski, H. Seidel	Perceptual Evaluation of Tone Mapping Operators with Regard to Similarity and Preference
MPI-I-2002-4-001	M. Goesele, J. Kautz, J. Lang, H.P.A. Lensch, H. Seidel	Tutorial Notes ACM SM 02 A Framework for the Acquisition, Processing and Interactive Display of High Quality 3D Models
MPI-I-2002-2-008	W. Charatonik, J. Talbot	Atomic Set Constraints with Projection
MPI-I-2002-2-007	W. Charatonik, H. Ganzinger	Symposium on the Effectiveness of Logic in Computer Science in Honour of Moshe Vardi
MPI-I-2002-1-008	P. Sanders, J.L. Trff	The Factor Algorithm for All-to-all Communication on Clusters of SMP Nodes
MPI-I-2002-1-005	M. Hoefer	Performance of heuristic and approximation algorithms for the uncapacitated facility location problem
MPI-I-2002-1-004	S. Hert, T. Polzin, L. Kettner, G. Schfer	Exp Lab A Tool Set for Computational Experiments
MPI-I-2002-1-003	I. Katriel, P. Sanders, J.L. Trff	A Practical Minimum Scanning Tree Algorithm Using the Cycle Property
MPI-I-2002-1-002	F. Grandoni	Incrementally maintaining the number of l-cliques
MPI-I-2002-1-001	T. Polzin, S. Vahdati	Using (sub)graphs of small width for solving the Steiner problem
MPI-I-2001-4-005	H.P.A. Lensch, M. Goesele, H. Seidel	A Framework for the Acquisition, Processing and Interactive Display of High Quality 3D Models